Energy & Environmental Science

Cite this: *Energy Environ. Sci.*, 2011, **4**, 2993

www.rsc.org/ees

PAPER

Proton exchange membrane electrolysis sustained by water vapor

Joshua M. Spurgeon and Nathan S. Lewis*

Received 21st February 2011, Accepted 19th April 2011
DOI: 10.1039/c1ee01203g

The current–voltage characteristics of a proton exchange membrane (PEM) electrolyzer constructed with an $IrRuO_x$ water oxidation catalyst and a Pt black water reduction catalyst, under operation with water vapor from a humidified carrier gas, have been investigated as a function of the gas flow rate, the relative humidity, and the presence of oxygen. The performance of the system with water vapor was also compared to the performance when the device was immersed in liquid water. With a humidified Ar(g) input stream at 20 °C, an electrolysis current density of 10 mA cm^{-2} was sustained at an applied voltage of ~1.6 V, with a current density of 20 mA cm^{-2} observed at ~1.7 V. In the system evaluated, at current densities >40 mA cm^{-2} the electrolysis of water vapor was limited by the mass flux of water to the PEM. At <40 mA cm^{-2}, the electrolysis of water vapor supported a given current density at a lower applied bias than did the electrolysis of liquid water. The relative humidity of the input carrier gas strongly affected the current–voltage behavior, with lower electrolysis current density attributed to dehydration of the PEM at reduced humidity values. The results provide a proof-of-concept that, with sufficiently active catalysts, an efficient solar photoelectrolyzer could be operated only with water vapor as the feedstock, even at the low operating temperatures that may result in the absence of active heating. This approach therefore offers a route to avoid the light attenuation and mass transport limitations that are associated with bubble formation in these systems.

I. Introduction

The membrane-based electrolysis of water is similar in concept, but differs significantly in operational detail, from the sunlight-driven membrane-based photoelectrolysis of water.[1–13] Specifically, to minimize capital expenditures, water electrolyzers are typically operated at high (>1 A cm^{-2} at 80–90 °C) current densities.[2,8] In contrast, the unconcentrated solar photon flux would limit, under optimal operating conditions, the current density of an integrated membrane-based water photoelectrolysis device, in which electrocatalysts embedded in a membrane are deposited onto the surface of light-absorbing semiconductor structures, to <20 mA cm^{-2}.[12,13] A second practical difference involves the impact of gas bubbles on the operation of the device. The flow of gas bubbles can provide active transport of liquid water to the surface of the electrodes, but bubble production can also deleteriously affect the steady-state current density at a given potential by reducing the contact area between the water and the electrocatalyst at either the anode or the cathode of an electrolysis unit. The production of

Joint Center for Artificial Photosynthesis, California Institute of Technology, Division of Chemistry and Chemical Engineering, 1200 E. California Blvd. m/c 127-72, Pasadena, CA, 91125, USA. E-mail: nslewis@caltech.edu

Broader context

One of the largest challenges to the global deployment of solar energy as a major resource is the intermittency of the sun. To overcome this obstacle, an inexpensive, efficient method is needed to store solar energy. Ideally, this storage would be in an energy-dense, portable form such as a fuel. The formation of hydrogen through water electrolysis is one viable approach for solar fuel production on a global scale. Although photovoltaic modules can be connected to conventional electrolyzers to split water, photoelectrolysis systems, in which sunlight is absorbed and the energy directly converted to decompose water to hydrogen and oxygen, have the potential to be more inexpensive and efficient. An efficient photoelectrolyzer, however, tends to limit its own performance by the formation of copious bubbles of gaseous products that inhibit the process by reflecting light and slowing the transfer of water to the catalyst reaction sites. Without concentrators, the intensity of the solar photon flux limits photoelectrolyzers to far lower current densities than are used in conventional electrolyzers. The work described herein demonstrates the feasibility of avoiding bubble formation issues by demonstrating that water vapor can be electrolyzed at room temperature at current densities in excess of those produced by the best photoelectrolysis systems.

bubbles is potentially of additional significance in a membrane-based photoelectrolysis system because the bubbles can refract and/or scatter the incoming incident illumination away from the photoactive electrode, thereby deleteriously affecting the overall performance of the solar-driven water electrolysis system.[12] Hence, strategies to minimize the effects of, or avoid completely, the formation of H_2 and O_2 bubbles during the electrolysis of water are highly desirable.

The use of water vapor as the system input feedstock, as opposed to liquid water, would completely eliminate any deleterious effects associated with the formation of H_2 or O_2 bubbles during water photoelectrolysis. A water vapor feedstock is problematic for conventional electrolyzers due to the resultant mass transport limitations of reactant at the current densities at which electrolysis systems are typically operated. Such a constraint is, however, greatly relaxed at the hundred-fold lower current densities that will be produced by membrane-based sunlight-driven photoelectrolysis systems operated under unconcentrated sunlight. In this work, we have therefore explored the performance limitations, if any, that would accompany the use of water vapor, instead of liquid water, as a feedstock in a solar-driven membrane-bound photoelectrolysis system.

We have used a commercially available, membrane-based water electrolysis unit as a demonstration system to evaluate any mass-transport limitations that would be associated with the use of water vapor instead of liquid water as the feedstock (Fig. 1). Water electrolysis based on catalyst-coated Nafion®-type sulfonated tetrafluoroethylene based fluoropolymer–copolymer proton exchange membranes (PEMs) is well-characterized both experimentally and operationally, being in essence the operational reverse of a PEM-based H_2/O_2 fuel cell.[2–8,14] However, little work has been reported to date on the use of gaseous water vapor as the feedstock to such electrolyzers.[15,16] Sawada *et al.* have demonstrated the feasibility of the concept,[16] but have not elucidated the effects of relative humidity (RH) or ambient temperature conditions on the performance of the electrolyzer. The system studied also did not use the best available catalysts and therefore could not definitively allow evaluation of any change in overpotentials that might occur when water vapor was used instead of liquid water. In our work, we have used a PEM electrolyzer that contained a Nafion membrane and highly active water oxidation and water reduction catalysts,[8–11] to investigate the changes in overpotential, as well as the mass transport limitations, that are associated with the substitution of water vapor for liquid water as the feedstock for such electrolyzer systems. We describe herein that, with active catalysts and with a well-hydrated membrane, an electrolysis current density of >20 mA cm^{-2} can be sustained at room temperature (20 °C) by the use of water vapor as a feedstock, and we also show that relatively little change in the performance of the electrolysis unit results, at moderate current densities, when water-saturated inert gas is used instead of liquid water as the electrolyzer feedstock.

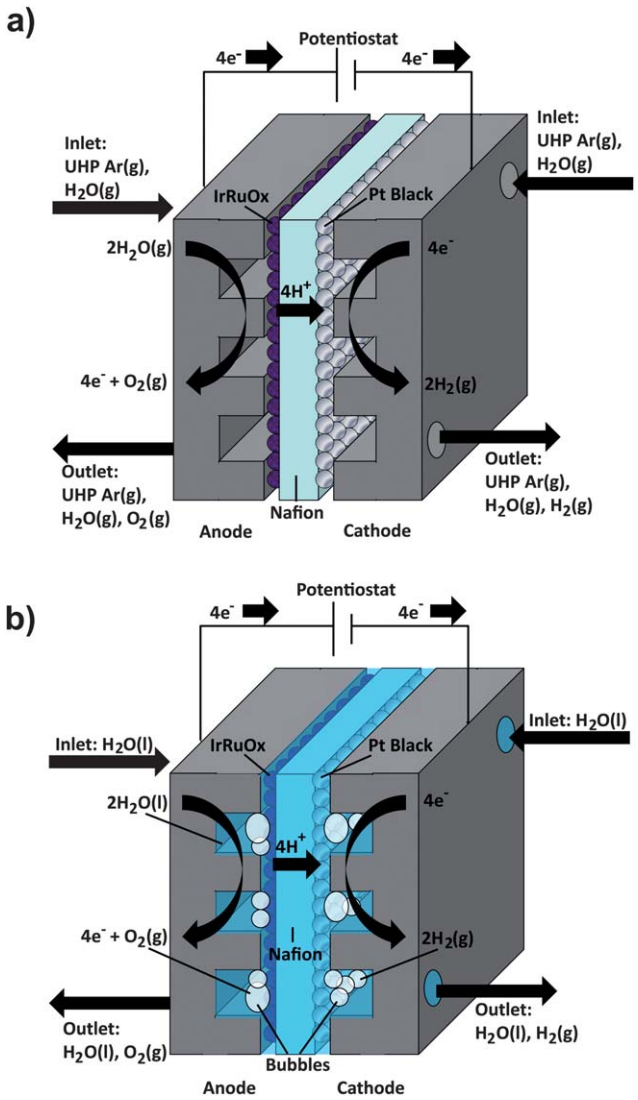

Fig. 1 Schematic of a cross-section of the electrolyzer under operation with (a) water vapor in UHP Ar(g) carrier gas as the feedstock and (b) liquid water as the feedstock. The product gases will form bubbles in liquid water, but bubble formation will be absent when water vapor is used as the electrolysis feedstock.

II. Experimental

A. PEM electrolyzer system

A commercially available demonstration fuel cell (Clean Fuel Cell Energy, LLC) system was used to construct the electrolyzer apparatus. The electrolyzer consisted of two graphite end plates (one for the anode and one for the cathode) that had serpentine gas flow channels (1.8 mm wide, 2.0 mm deep, spaced 1.0 mm apart, which, including the inlet and outlet ports, resulted in ~80% of the active area of the membrane being directly exposed to the input gas flow) grooved into the side of the plate that faced the membrane. The membrane was Nafion (Lynntech, Nafion 115, 127 μm thick) that had an anode catalyst loading of 3.0 mg cm^{-2} of $IrRuO_x$ (1 : 1, IrO_2 : RuO_2) and a cathode catalyst loading of 3.0 mg cm^{-2} of Pt black. The projected active area of the membrane was 5 cm^2. Gas diffusion layers were not used, due to the instability under electrolysis conditions of the carbon-based material in a typical gas diffusion layer.

Ultra-high purity (UHP) Ar(g) (>99.99%) was used as the carrier gas in all experiments, except for the specifically identified experiments in which the carrier gas was either N_2(g) (>99.99%)

or house air (1.10 ± 0.15 ppth of water vapor). The carrier gas was saturated with water vapor by passing the gas at a flow rate of 0.04–0.5 L min^{-1} (controlled by flow meters from Chemglass) through a bubbler that had been filled with 18 MΩ cm resistivity deionized H_2O, obtained from a Barnstead Nanopure system. The humidified gas stream was mixed with a dry gas stream, both at controlled flow rates, to create a gas flow of the desired relative humidity (RH). The system produced precise (±2% RH) and reproducible humidity values in the gas flow stream, as monitored by a relative humidity probe (Omega, RH-USB sensor). A water-saturated carrier gas stream to which dry gas had not been added had RH of ~95%. To minimize the back diffusion of ambient oxygen into the electrolysis unit, the output stream from the electrolyzer was bubbled through an oil bath. For the electrolysis of liquid water, the electrolyzer cell was immersed in 18 MΩ cm resistivity $H_2O(l)$ that had been deoxygenated by bubbling with Ar(g) for >1 h. All experiments were conducted at an ambient temperature of 20 °C.

B. Data collection

Before measurement of the current density–voltage (*J*–*V*) behavior under each set of experimental conditions (flow rate, RH, *etc.*), the electrolyzer was allowed to equilibrate at open circuit for >2 h. An SI model 1286 Schlumberger potentiostat was used to apply a DC bias to the electrolyzer cell, and to measure the current through the cell, through current collector pins in contact with each of the graphite end plates of the electrolysis unit. The current reached an approximate steady state value after >300 s at each applied bias. The *J*–*V* behavior was also measured by sweeping the voltage, at a scan rate of 1 mV s^{-1}, from open circuit to 2.6 V. The current values measured at a given potential in the scan were in close agreement with the current that was measured at that same potential after 300 s under potentiostatic conditions. The current density was determined using the full projected area of the active part of the membrane electrode assembly (5 cm^2).

III. Results

A. Gaseous *vs.* liquid water feedstocks

Fig. 2 depicts the *J*–*V* behavior of the electrolyzer with liquid water as a feedstock relative to the behavior observed with a flow of Ar(g) saturated with water vapor as the feedstock. For $V < 2$ V (*i.e.*, $J < 30$ mA cm^{-2}), the performance was very similar in both cases, and at a given voltage more current was observed with water vapor as the feedstock than with liquid water as the feedstock. The limiting electrolysis current density increased with increasing Ar(g)/H_2O(g) flow rate, from a value of ~25 mA cm^{-2} at 0.05 L min^{-1} to ~40 mA cm^{-2} at a flow rate of 0.3 L min^{-1} to each electrode (Fig. 2). In contrast, when immersed in liquid water, the electrolyzer did not reach a limiting current density within the experimentally measured voltage range, with the current density exceeding 70 mA cm^{-2} at $V = 2.5$ V at 20 °C.

B. Relative humidity

Variations in the RH of the input carrier gas stream significantly affected the *J*–*V* behavior of the electrolyzer. When the RH was

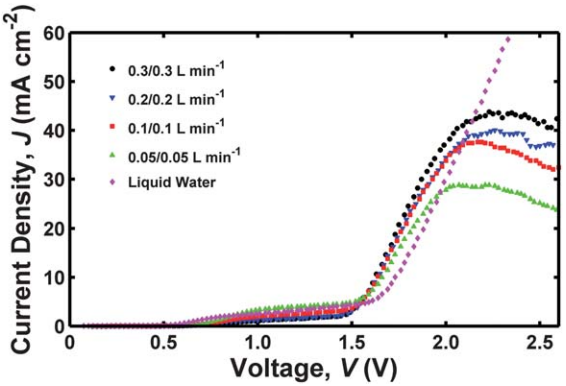

Fig. 2 Plot of current density, *J*, *vs.* applied voltage, *V*, when varying the carrier gas flow rate. In the legend, the information provided is for the anode/cathode, specifying the gas flow rate to each electrode. The carrier gas was UHP Ar(g) with RH = 95% in each case, and the operating temperature was 20 °C. The data represented by pink diamonds are the *J*–*V* behavior of the electrolyzer immersed in liquid water at 20 °C.

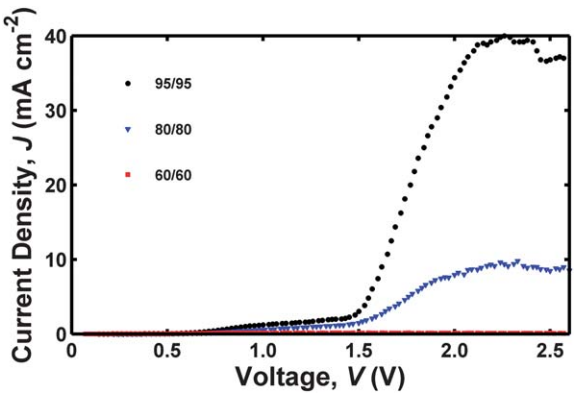

Fig. 3 Plot of current density, *J*, *vs.* applied voltage, *V*, when varying the RH. In the legend, the information provided is for the anode/cathode, specifying the RH of the gas stream to each electrode. The carrier gas was UHP Ar(g) at a flow rate of 0.2 L min^{-1} in each case, and the operating temperature was 20 °C.

decreased equally to each electrode (Fig. 3), the current density dropped precipitously, with negligible electrolysis current sustained at RH ≤60%. The decline in performance was less severe when the gas was fully humidified to one electrode in the system. A reduction in the water content of the gas feed was somewhat more tolerable when only the RH to the cathode gas feed was varied, with a non-negligible electrolysis current requiring RH ≥20% (Fig. 4), as compared to when the RH in the gas feed to the anode was varied, in which case a non-negligible electrolysis current required RH ≥40% (Fig. 5) in the input feed at 20 °C.

C. Presence of O_2 in the input gas stream

Fig. 6 shows the effect on the *J*–*V* behavior of using humidified air, Ar(g), or N_2(g) as the carrier gas to the anode and/or cathode of the electrolyzer. No significant difference was observed in the *J*–*V* performance of the electrolyzer when the carrier gas introduced to both electrodes was changed from Ar(g) to N_2(g). In both cases, the current density remained low ($J < 2$ mA cm^{-2})

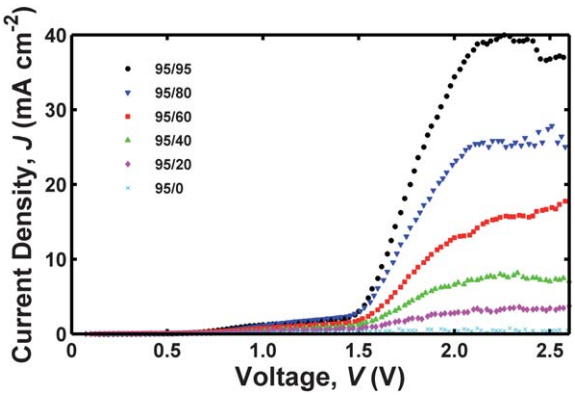

Fig. 4 Plot of current density, J, *vs.* applied voltage, V, when varying the RH in the cathode gas stream. In the legend, the information provided is for the anode/cathode, specifying the RH of the gas stream to each electrode. The carrier gas was UHP Ar(g) at a flow rate of 0.2 L min^{-1} in each case, and the operating temperature was 20 °C.

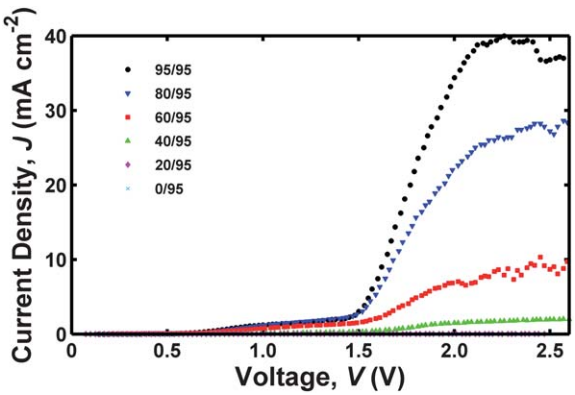

Fig. 5 Plot of current density, J, *vs.* applied voltage, V, when varying the RH in the anode gas stream. In the legend, the information provided is for the anode/cathode, specifying the RH of the gas stream to each electrode. The carrier gas was UHP Ar(g) at a flow rate of 0.2 L min^{-1} in each case, and the operating temperature was 20 °C.

until $V > 1.5$ V, at which point the current density increased rapidly, reaching values of 10 mA cm^{-2} at ~1.6 V and 20 mA cm^{-2} at ~1.7 V. For $V >$ ~2.1 V, the current density plateaued at ~35 to 40 mA cm^{-2}.

Nearly identical behavior was observed when air was supplied to the anode and an inert gas was supplied to the cathode. However, use of air as the carrier gas introduced to the cathode, with either an inert gas or air introduced to the anode, produced a significant increase in J for $V < 1.5$ V. Specifically, with air flowing to the cathode, $J = 10$ mA cm^{-2} was observed at $V \approx 1.0$ V, and $J = 20$ mA cm^{-2} was observed at ~1.2 V. For $V > 1.5$ V, the current density remained at ~40 to 45 mA cm^{-2}.

IV. Discussion

A. Gaseous *vs.* liquid water inputs

The experiments demonstrate that electrolysis in a membrane-based system can clearly be sustained at $J = 10$–20 mA cm^{-2} with water vapor as the feedstock. The flux of water molecules to the membrane became a limiting factor at higher current densities.

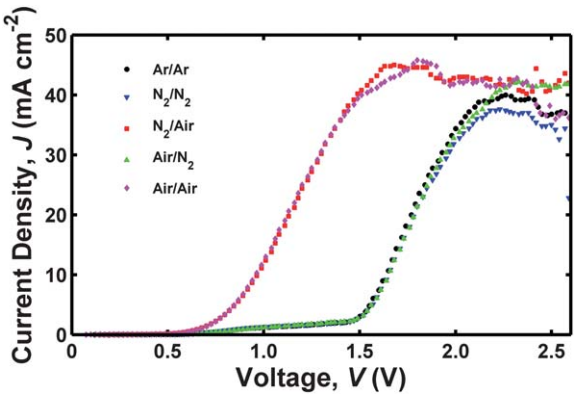

Fig. 6 Plot of current density, J, *vs.* applied voltage, V, when using either air or inert carrier gas. In the legend, the information provided is for the anode/cathode, specifying which carrier gas was supplied to each electrode. The gas flow rate was 0.2 L min^{-1} at RH = 95% to each electrode, and the operating temperature was 20 °C.

Higher flow rates of humidified gas to the electrolyzer resulted in an increased mass flux of water to the membrane surface, reducing the effect of mass transport limitations. Increasing the flow rate of humidified Ar(g) to each electrode, from 0.05 L min^{-1} to 0.3 L min^{-1}, increased the limiting electrolysis current density by ~60% (from 25 mA cm^{-2} to 40 mA cm^{-2}). For a given photoelectrolysis system with semiconductor light absorbers producing a set photovoltage and with an overpotential dependent upon the catalysts employed, the active flow of humidified gas to the electrodes could be optimized to reach the maximum attainable current density without an unnecessarily high flow rate. We also note that our observations are lower bounds on the attainable current density in such a system because no gas diffusion layer was used and the graphite end plates were directly attached to the catalyst layer, so only the portion (~80%) of the catalyst that was directly exposed to the gases, and then only the fraction that was within useful electrical contact laterally to the electrodes, was electrochemically active as configured in this test system.

In the presence of highly active electrocatalysts, the onset of significant electrolysis current density occurred at a higher voltage for liquid, rather than gaseous, water as the feedstock (Fig. 2). At 20 mA cm^{-2}, this difference resulted in a ~140 mV discrepancy between the applied bias required under a flow rate of 0.2 L min^{-1} of humidified Ar(g) relative to the applied bias required using liquid water. The reduced voltage required for electrolysis when using water vapor can be partially attributed to the difference in ΔG_f^0 (standard Gibbs free energy of formation) between liquid water and gaseous water, with ΔG_f^0 [H_2O(l)] = −237.18 kJ mol^{-1}, and ΔG_f^0 [H_2O(g)] = −228.59 kJ mol^{-1}.[17] The ΔG^0 relates to the standard potential of the cell reaction, E^0, by:[18]

$$\Delta G^0 = -nFE^0 \quad (1)$$

where n is the number of electrons passed per H_2O molecule reacted ($n = 2$), and F is Faraday's constant ($F = 96\,485$ C mol^{-1}). This equation results in thermodynamic water-splitting potentials of E^0 [H_2O(l)] = 1.229 V and E^0 [H_2O(g)] = 1.185 V. Therefore, in the thermodynamic limit, the electrolysis of liquid water requires an extra 44 mV of bias as compared to the

electrolysis of water vapor. This difference only partially accounts for the observed shift in the *J–V* behavior between electrolysis with $H_2O(l)$ *vs.* $H_2O(g)$ as the feedstock. The remaining voltage difference is attributed, at least in part, to a reduced contact area between liquid water and the catalyst due to bubble formation. Additionally, part of the voltage shift between gaseous *vs.* liquid water inputs may be due to a change in the catalytic overpotential, due to the different local environments at the membrane surface under these different conditions. This shift in the voltage for electrolysis indicates that when low current densities are required ($\leq$20 mA cm^{-2}), the use of water vapor may be preferable to liquid water as the feedstock. Notably, the fuel cell employed in this work was not an ideal electrolyzer, and the use of a more optimized device may yield further increases in performance for both liquid and gaseous water feedstocks.

B. Relative humidity

The effect of the RH of the gas stream on the *J–V* behavior is an important factor when assessing the tolerance of the electrolyzer to ambient conditions. Fig. 3 shows that even a minor decrease in RH at 20 °C produced a significant decrease in electrolyzer performance, with no observable current at a RH of $\leq$60%. The steep drop in the *J–V* behavior of the electrolyzer with RH is likely due to dehydration of the membrane. Nafion must be kept well-hydrated to maintain its high ionic conductivity because water preferentially fills hydrophilic, negatively charged channels which then enable the selective transfer of protons.[14,19] Without sufficient water, the channels constrict and the membrane conductivity is significantly reduced. The lower the RH is below 100%, the more moisture from the membrane will evaporate, decreasing the conductivity and affecting the steady state *J–V* behavior of the electrolyzer.

Although the difference between the *J–V* behavior with reduced humidity at the cathode (Fig. 4) and the *J–V* behavior with reduced humidity at the anode (Fig. 5) was fairly minor, the electrolyzer performed somewhat better when the low RH values ($\leq$60%) were at the cathode. This is consistent with expectations, because the decomposition of H_2O molecules occurs at the anode. Low water content at the anode would thus be expected to have a more pronounced effect on the *J–V* behavior of the system than low water content at the cathode. Clearly, providing a fully humidified feed to one electrode partially mitigated the membrane drying effect relative to the case of reduced humidity to both electrodes (Fig. 3). If the membrane can be kept well-hydrated, it may be possible to sustain the *J–V* behavior similar to that shown in Fig. 2 even with lower RH in the input gas streams. This hydration may be possible by periodically or continually sprinkling or misting the membrane with water. Alternatively, a Nafion membrane could be fabricated with a web of hydroponic polymer integrated into it that would wick water from a reservoir at the side of the water-splitting device.

C. Presence of O_2 in the input gas stream

To produce the most economically viable solar fuel generation device, photoelectrolysis should operate with minimal active input to the system—*i.e.*, passive heating only and little to no required pumping of reactants. Ideally, fuel could be produced simply by photoelectrolyzing water vapor directly from the ambient atmosphere. As shown in Fig. 6, the introduction of air to the anode alone did not result in any noticeable change to the *J–V* behavior of the electrolyzer as compared to its performance under humidified inert gas. Because $O_2(g)$ is produced at the anode during water-splitting, the addition of $O_2(g)$ in air to the carrier gas feed thus has no further effect on the behavior of the electrolyzer. However, the presence of $O_2(g)$ in air at the cathode had a strong effect on the *J–V* behavior of the electrolyzer (Fig. 6). Under these conditions, the cathode is essentially performing the opposite reaction to the anode, reducing $O_2(g)$ back into water by combining $O_2(g)$ with protons coming from the membrane. The onset of current occurred for $V > 500$ mV, rather than at 0 V, due to the catalytic overpotential. Thus, because the reduction of $O_2(g)$ is thermodynamically favored relative to $H_2(g)$ evolution, the steady-state flux of $O_2(g)$ to the catalyst sites at the cathode will need to be kept low to prevent $O_2(g)$ reduction from significantly impairing the overall cell efficiency. At >1.5 V, $H_2(g)$ evolution will occur at the cathode as well, competing kinetically with $O_2(g)$ reduction in consuming protons. If $H_2(g)$ is produced rapidly enough relative to the input air flow rate, the $H_2(g)$ could purge the $O_2(g)$ from the catalyst surface, ensuring maximum $H_2(g)$ production. Of course, the $H_2(g)$ will need to be separated from any $O_2(g)$ in the cathode effluent downstream before the gases recombine to form water. If no $O_2(g)$ is input to the cathode, the cathode should self-purge and become depleted of $O_2(g)$, except for the steady-state $O_2(g)$ crossover from the anode. Therefore, while it is clearly possible to expose the anode of a water vapor photoelectrolysis system to the atmosphere during operation in the field, the introduction of air to the cathode is only feasible under conditions for which the reduction of $O_2(g)$ is not replacing the evolution of $H_2(g)$. Further research is required to determine the flow rates and reactor designs that might optimize this mode of operation.

To ensure that the observed *J–V* behavior was due exclusively to splitting water, UHP Ar(g) was the sole carrier gas used in all other experiments reported herein. Bubbling the output gas stream through an oil bath was necessary to prevent the diffusion of ambient oxygen into the cathode compartment. Any remaining nonzero current observed at voltages <1.23 V can thus be attributed to ambient $O_2(g)$ diffusing directly into the demonstration fuel cell that served as the electrolyzer.

D. Temperature

Because an inexpensive photoelectrolysis device will likely not include active heating, the experiments reported herein were all conducted at a relatively low temperature (20 °C) for electrolysis. Passive heating elements (*i.e.*, a black body layer to produce heat by collecting light not absorbed by the semiconductor components), however, may enable operation at higher than ambient temperatures. Previous experimental results and electrolyzer models based on Butler–Volmer kinetics indicate that increased temperature will lead to higher current densities for a given applied bias.[15,16] Additionally, fully humidified gas at higher temperature has a greater water content, which may raise the limiting current density of electrolysis sustained by water vapor. The current densities reported herein should therefore be

considered to be the lower bounds attainable with active water oxidation and reduction catalysts, but these values may be particularly relevant for evaluating the system operation with passive heating of the device in cooler climates. Initial experiments indicated that water management and hydration of the membrane became increasingly critical at higher operating temperatures, with RH <100% leading to membrane dehydration, and consequently to a large decrease in the electrolysis current density. The operation of an electrolyzer with water vapor at higher temperatures may require a scheme to keep the Nafion hydrated or the use of an alternative ionomer that is less sensitive to its water content.

E. System engineering considerations

The ability to operate on a water vapor feedstock could ease the system engineering constraints associated with a PEM-based photoelectrolyzer. In a complete, membrane-integrated device, however, light must be managed and optimally distributed between the semiconductor photoanode and photocathode without significant absorption losses to the catalysts or membrane, and all materials must be stable at the pH of the operating environment. The membrane must incorporate and support the semiconductor components, electrically connect the photoanode to the photocathode, exchange ions to prevent the buildup of a pH gradient, separate the gaseous reaction products, and be transparent to the above-band gap illumination.[20] Additionally, in a liquid environment, the device would need to be engineered to minimize bubble trapping at the semiconductor/catalyst surface. Operation in a gaseous environment eliminates this issue; however, high surface area semiconductor electrodes will likely need to be covered with a polymer electrolyte to maximize the three-phase contact area.

V. Conclusion

PEM electrolysis has been sustained using water vapor at current densities sufficient to support an efficient photoelectrolysis system operating under 1 Sun illumination. It should therefore be possible to avoid the disadvantageous effects of bubble formation during operation of a solar fuel generation device by utilizing gaseous, rather than liquid, water as the feedstock. At 20 °C with an $IrRuO_x$ water oxidation catalyst and a Pt black reduction catalyst, an applied bias of ~1.7 V resulted in a current density of 20 mA cm^{-2}. Under these conditions, a water vapor feedstock supported electrolysis current densities <30 mA cm^{-2} at a lower applied bias than was required to attain the same current density in liquid water. Decreasing the RH in the input carrier gas stream strongly degraded the electrolyzer performance, most likely due to dehydration of the Nafion membrane. If the membrane can be kept well-hydrated, it may be possible to sustain electrolysis by exposing the electrodes to ambient water vapor in air; however, the air flow rate to the cathode should be carefully chosen to prevent O_2(g) reduction from significantly decreasing the H_2(g) evolution rate.

Acknowledgements

This work was performed by the Joint Center for Artificial Photosynthesis, a DOE Energy Innovation Hub that is supported through the Office of Science of the U.S. Department of Energy under Award Number DE-SC0004993. We acknowledge use of facilities supported by the Caltech Center for Science and Engineering of Materials, an NSF MRSEC, and the Caltech Center for Sustainable Energy Research.

References

1 R. J. Davenport, F. H. Schubert and D. J. Grigger, *J. Power Sources*, 1991, **36**, 235–250.
2 S. A. Grigoriev, V. I. Porembsky and V. N. Fateev, *Int. J. Hydrogen Energy*, 2006, **31**, 171–175.
3 S. P. S. Badwal, S. Giddey and F. T. Ciacchi, *Ionics*, 2006, **12**, 7–14.
4 L. L. Swette, A. B. Laconti and S. A. McCatty, *J. Power Sources*, 1994, **47**, 343–351.
5 F. Barbir, *Sol. Energy*, 2005, **78**, 661–669.
6 P. H. Choi, D. G. Bessarabov and R. Datta, *Solid State Ionics*, 2004, **175**, 535–539.
7 J. H. Nie, Y. T. Chen, R. F. Boehm and S. Katukota, *J. Heat Transfer*, 2008, **130**, 042409.
8 Y. J. Zhang, C. Wang, N. F. Wan and Z. Q. Mao, *Int. J. Hydrogen Energy*, 2007, **32**, 400–404.
9 M. G. Walter, E. L. Warren, J. R. McKone, S. W. Boettcher, Q. X. Mi, E. A. Santori and N. S. Lewis, *Chem. Rev.*, 2010, **110**, 6446–6473.
10 E. Slavcheva, I. Radev, S. Bliznakov, G. Topalov, P. Andreev and E. Budevski, *Electrochim. Acta*, 2007, **52**, 3889–3894.
11 A. Di Blasi, C. D'Urso, V. Baglio, V. Antonucci, A. S. Arico, R. Ornelas, F. Matteucci, G. Orozco, D. Beltran, Y. Meas and L. G. Arriaga, *J. Appl. Electrochem.*, 2009, **39**, 191–196.
12 O. Khaselev and J. A. Turner, *Science*, 1998, **280**, 425–427.
13 S. Licht, B. Wang, S. Mukerji, T. Soga, M. Umeno and H. Tributsch, *J. Phys. Chem. B*, 2000, **104**, 8920–8924.
14 J. Larminie and A. Dicks, *Fuel Cell Systems Explained*, John Wiley & Sons, West Sussex, England, 2nd edn, 2003.
15 S. D. Greenway, E. B. Fox and A. A. Ekechukwu, *Int. J. Hydrogen Energy*, 2009, **34**, 6603–6608.
16 S. Sawada, T. Yamaki, T. Maeno, M. Asano, A. Suzuki, T. Terai and Y. Maekawa, *Prog. Nucl. Energy*, 2008, **50**, 443–448.
17 D. W. Oxtoby, H. P. Gillis and N. H. Nachtrieb, *Principles of Modern Chemistry*, Saunders College Publishing, Orlando, FL, USA, 4th edn, 1999.
18 A. J. Bard and L. R. Faulkner, *Electrochemical Methods: Fundamentals and Applications*, John Wiley & Sons, 2nd edn, 2001.
19 C. Heitner-Wirguin, *J. Membr. Sci.*, 1996, **120**, 1–33.
20 J. M. Spurgeon, M. G. Walter, J. Zhou, P. A. Kohl and N. S. Lewis, *Energy Environ. Sci.*, 2011, **4**, 1772–1780.

